

The adhesion G-protein coupled receptor VLGR1/ADGRV1 controls autophagy

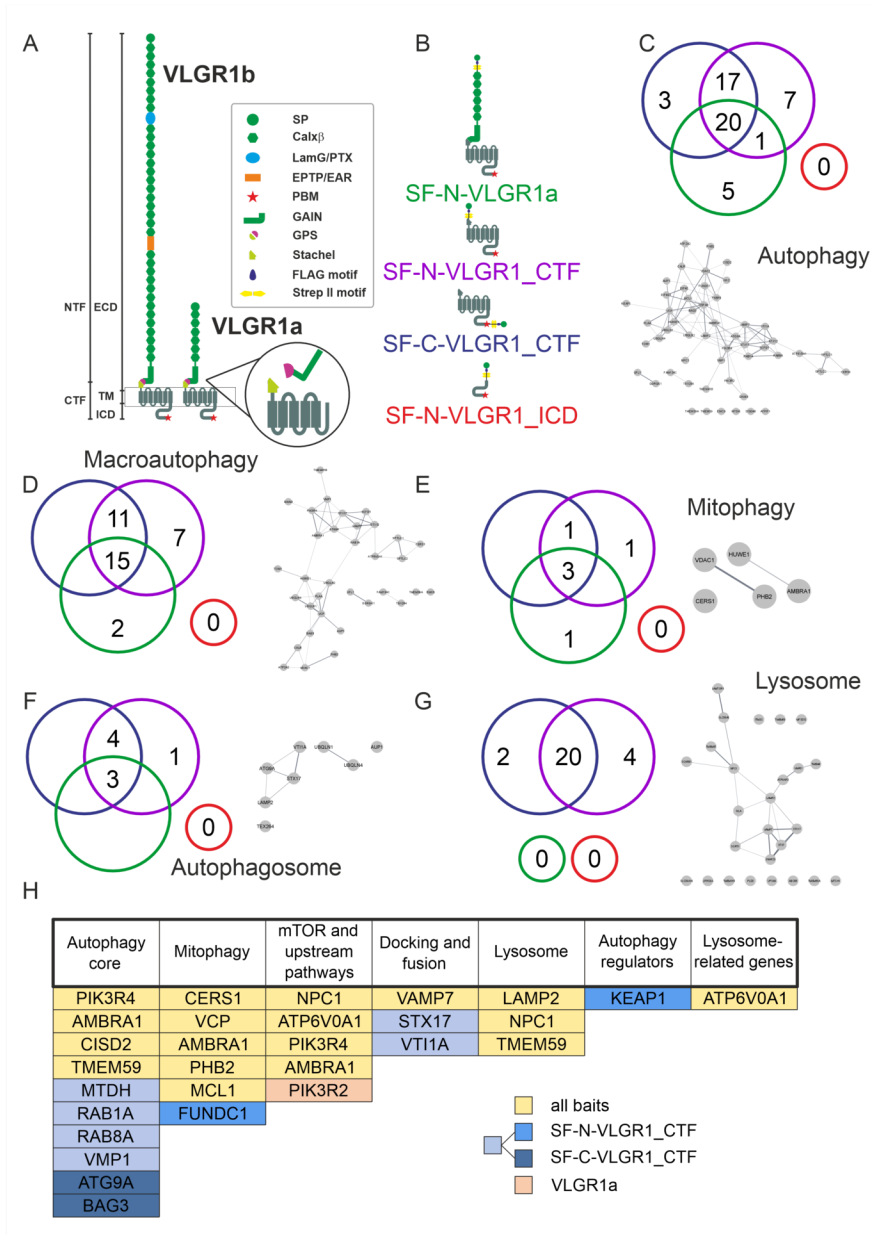
Joshua Linnert¹, Baran Güler¹, Jacek Krzysko¹, and Uwe Wolfrum¹

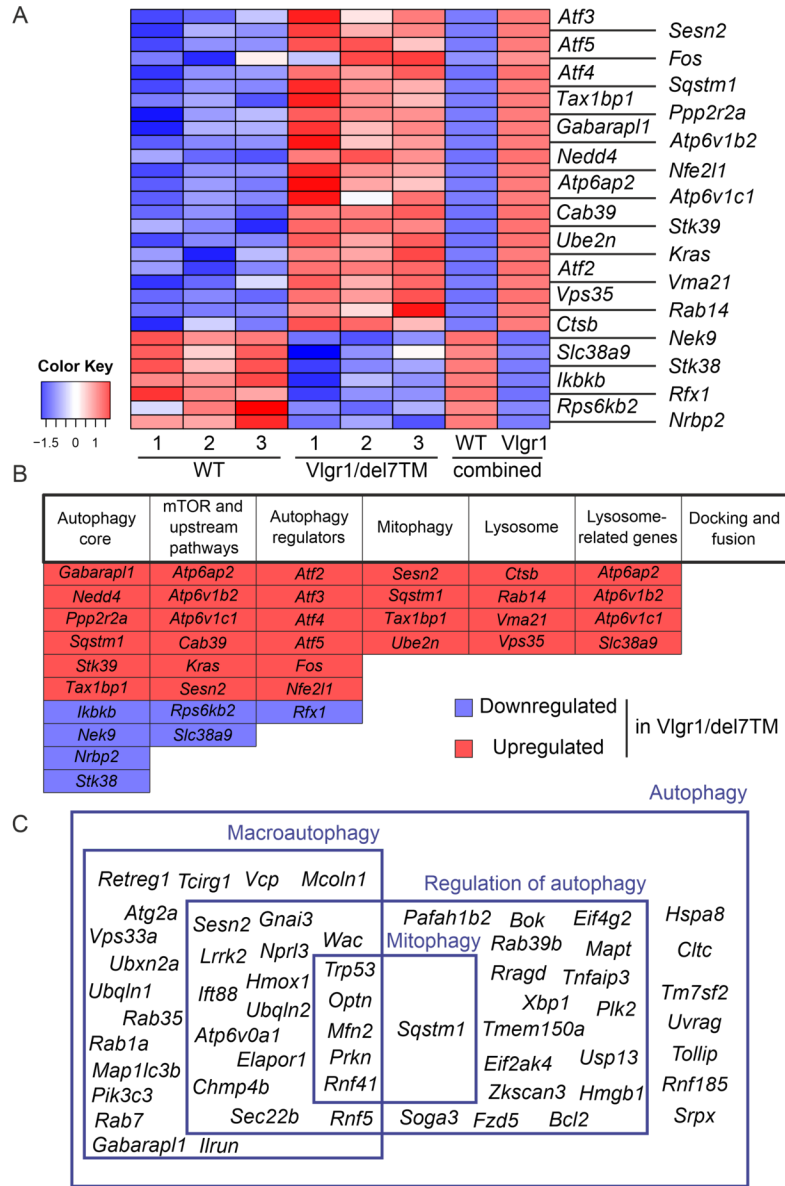
¹Johannes Gutenberg Universitat Mainz

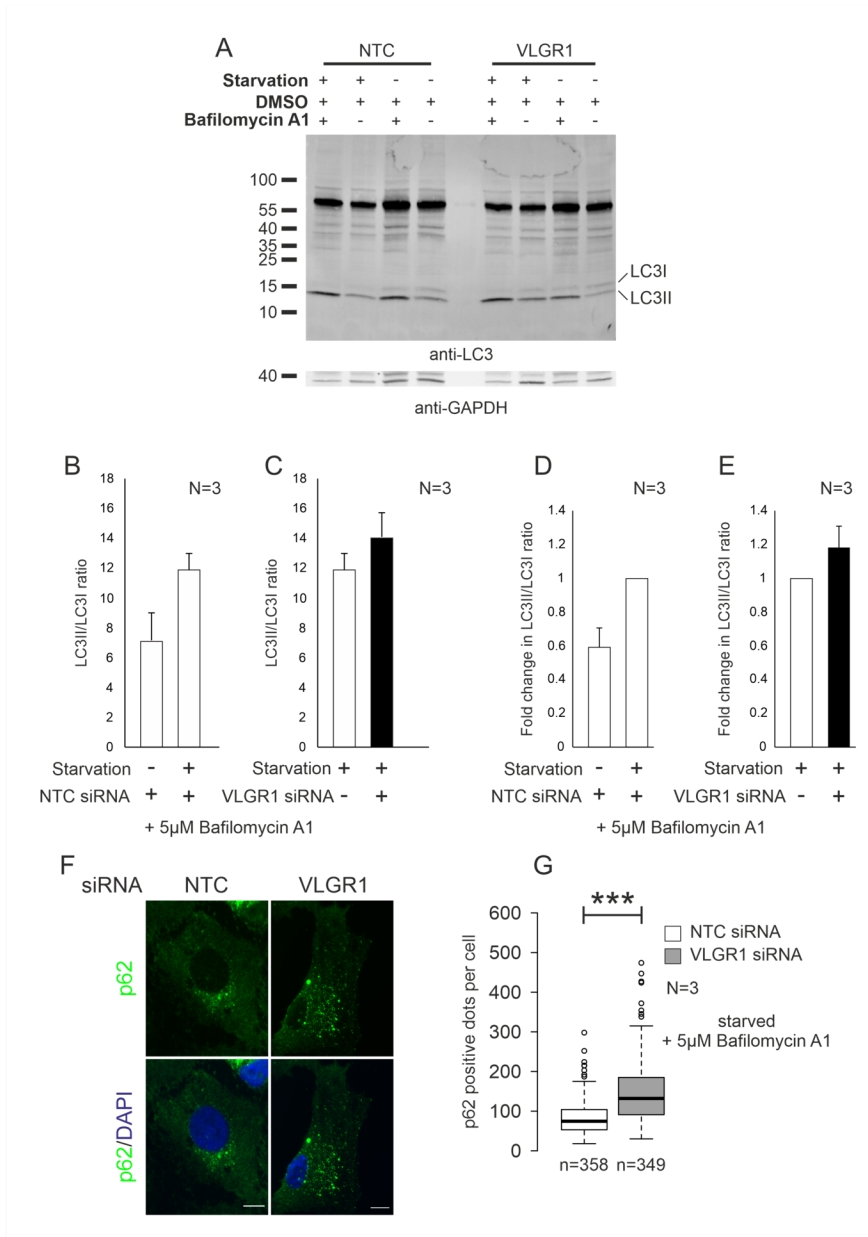
January 4, 2023

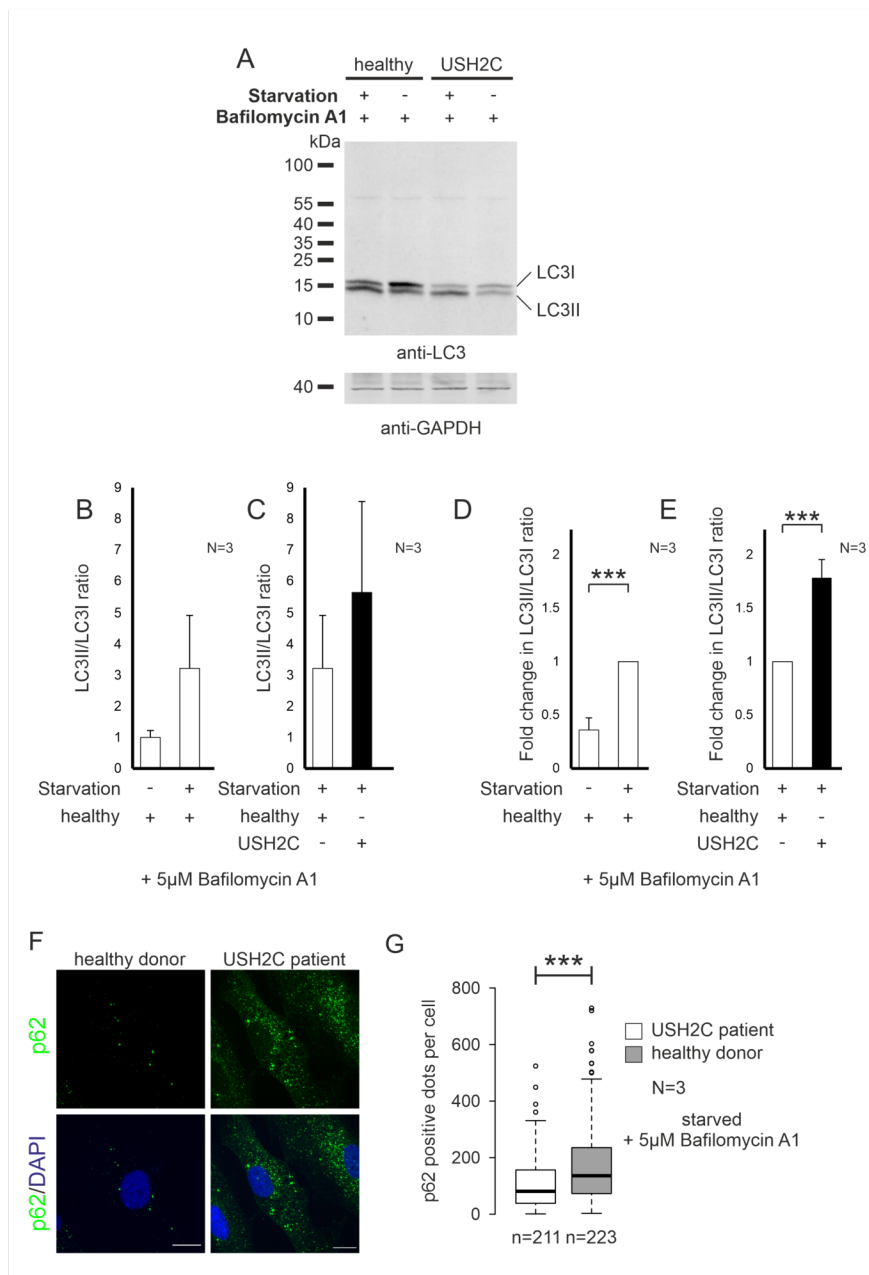
Abstract

VLGR1/ADGRV1 (very large G protein-coupled receptor-1) is the largest known adhesion G protein-coupled receptor. Mutations in VLGR1/ADGRV1 cause Usher syndrome (USH), the most common form of hereditary deaf-blindness, and have been additionally linked to epilepsy. Although VLGR1/ADGRV1 is almost ubiquitously expressed, little is known about the subcellular function and signalling of the VLGR1 protein and thus about mechanisms underlying the development of diseases. Using affinity proteomics, we have identified key components of autophagosomes as putative interacting proteins of VLGR1. In addition, whole transcriptome sequencing of the retinae of the *Vlgr1/del7TM* mouse model revealed altered expression profiles of gene-related autophagy. Monitoring autophagy by immunoblotting and immunocytochemistry of the LC3 and p62 as autophagy marker proteins revealed evoked autophagy in VLGR1-deficient hTERT-RPE1 cells and USH2C patient-derived fibroblasts. Our data demonstrate the molecular and functional interaction of VLGR1 with key components of the autophagy process and point to an essential role of VLGR1 in the regulation of autophagy at internal membranes. The close association of VLGR1 with autophagy helps to explain the pathomechanisms underlying human USH and epilepsy-related to VLGR1 defects.









The adhesion G-protein coupled receptor VLGR1/ADGRV1 controls autophagy

Joshua Linnert, Baran E. Güler, Jacek Krzysko, Uwe Wolfrum*

Institute of Molecular Physiology, Molecular Cell Biology, Johannes Gutenberg University
Mainz, 55128 Mainz, Germany.

*Corresponding author: Institute of Molecular Physiology, Molecular Cell Biology, Johannes
Gutenberg University Mainz, Hanns-Dieter-Hüsch-Weg 17, 55128 Mainz, Germany; e-mail:
wolfrum@uni-mainz.de

Keywords: Adhesion GPCR, Autophagy, Usher syndrome, affinity proteomics, proteostasis

Running title: VLGR1/ADGRV1 controls autophagy

Abstract

VLGR1/ADGRV1 (very large G protein-coupled receptor-1) is the largest known adhesion G protein-coupled receptor. Mutations in *VLGR1/ADGRV1* cause Usher syndrome (USH), the most common form of hereditary deaf-blindness, and have been additionally linked to epilepsy. Although VLGR1/ADGRV1 is almost ubiquitously expressed, little is known about the subcellular function and signalling of the VLGR1 protein and thus about mechanisms underlying the development of diseases.

Using affinity proteomics, we have identified key components of autophagosomes as putative interacting proteins of VLGR1. In addition, whole transcriptome sequencing of the retinae of the *Vlgr1/del7TM* mouse model revealed altered expression profiles of gene-related autophagy. Monitoring autophagy by immunoblotting and immunocytochemistry of the LC3 and p62 as autophagy marker proteins revealed evoked autophagy in VLGR1-deficient hTERT-RPE1 cells and USH2C patient-derived fibroblasts.

Our data demonstrate the molecular and functional interaction of VLGR1 with key components of the autophagy process and point to an essential role of VLGR1 in the regulation of autophagy at internal membranes. The close association of VLGR1 with autophagy helps to explain the pathomechanisms underlying human USH and epilepsy-related to VLGR1 defects.

1. Introduction

G protein-coupled receptors (GPCRs) are the most important receptors of our body as they respond to almost all external stimuli and therefore prime targets for pharmacological interventions. Although adhesion GPCRs (ADGRs) are the second largest subclass of GPCRs, their function is the least understood of all GPCR classes, so their pharmacological significance has also had to remain fairly unexplored. ADGRs are characterized by signature domains of serpentine (7TM) and adhesion proteins (Figure 1A). Among ADGRs the very large G protein-coupled receptor 1 (VLGR1), also named ADGRV1, GPR98 or MASS1 is the largest ^{1,2}. As other ADGRs, VLGR1 is composed of an extracellular N-terminal fragment (adhesion part), which is extremely long in VLGR1, fused by a GAIN domain, which includes the GPCR autoproteolytic cleavage site (GPS) to a C-terminal fragment defined by 7TM domain (receptor part) (Figure 1A). Evidence suggests that autocleavage at GPS exposes the short so-called "spike" sequence at the N-terminal end of CTF, which serves as a bound agonist to activate aGPCRs ^{3,4}. In VLGR1, we have recently identified 11 amino acids that act as the "Stachel" peptide⁵. Furthermore, we also found evidence that this activation induces a switch from Gs- to Gi-mediated signalling of VLGR1.

In mammals, VLGR1 is almost ubiquitously expressed, with high expression in the nervous system, especially in the neural cells of the developing brain and the sensory cells of the eye and inner ear ^{1,2,6} (Protein Atlas: <https://www.proteinatlas.org/>). Mutations in the *VLGR1/ADGRV1* gene cause Usher syndrome type 2C (USH2C) which is characterized by congenital sensorineural hearing loss and retinitis pigmentosa (RP) ⁷. Additionally, mutations, even haploinsufficiency of *VLGR1/ADGRV1* have been associated with different forms of epilepsy in humans and audiogenic seizures in mice (Dahawi et al. 2021; Myers et al. 2018; Zhou et al. 2022). Almost nothing is known to date about the pathomechanisms underlying epileptogenesis that lead to the imbalance between excitatory and inhibitory neurotransmission described in epilepsy patients. In the two sensory cell types affected in USH type 2, retinal photoreceptor cells and cochlear hair cells, VLGR1 is essential for the formation of filamentous connections between membranes, namely the membranes of the connecting cilium and the inner segment in photoreceptor cells and ankle-links connecting adjacent stereocilia in differentiating hair bundles of the cochlear hair cells ^{1,6,10,11}. The absence of VLGR1 leads to a disturbance of membrane-membrane adhesion, which is manifested by the conspicuous disorganization of the stereotypic arrangement of stereocilia in the hair bundles in the hair cells. However, it remains

unknown whether, in addition to these apparent defects in adhesion, altered G protein-coupled signalling contributes to the pathophysiology of sensory cells in USH2C.

Because knowledge of potential interaction partners often provides reliable insights into the function of proteins, we have searched for potential partners of VLGR1 by an affinity proteomics capture approach to provide insights into its cellular functions^{5,12}. This strategy has recently enabled us to unravel valuable new insights into the downstream receptor signalling of VLGR1⁵, its participation as a metabotropic membrane mechanoreceptor in the regulation of focal adhesion during cell migration^{13,14}, and its role in the function of internal membrane compartments, such as the mitochondria-associated membranes (MAMs) of the endoplasmic reticulum (ER)¹⁵. The absence of VLGR1 results in a disturbance in the MAM architecture and the dysregulation of the Ca²⁺ transient from ER to mitochondria¹⁵. MAMs are nuclei for autophagosomes in the autophagy process¹⁶, the intracellular degradation system for cytoplasmic contents, e.g., for defective intracellular proteins, excess or damaged organelles, or invaded microorganisms¹⁷⁻²⁰. Classical autophagy also named as macroautophagy is characterized by sequential steps, such as the formation of autophagosomes from the phagophore and the fusion with lysosomes leading to digestive autolysosomes^{17,21}. There are also several subtypes of autophagy, for instance chaperone-mediated autophagy is mainly based on the interaction of heat shock proteins with proteins determined for degradation^{17,18}. Also, autophagy of whole organelles such as mitochondria or the ER are defined as mitophagy or ER-phagy, respectively²²⁻²⁴. Defects in autophagy can evoke or exacerbate diseases namely neurodegenerative diseases such as Huntington, Alzheimer's or retinal degeneration²⁵⁻²⁷.

Here, we show that the adhesion GPCR VLGR1 interacts with core components of autophagy and that in the absence of VLGR1, autophagy activities increase, leading to differential expression of autophagy-related genes. This close association of VLGR1 with the autophagy process may help to explain the pathomechanisms underlying the diseases related to VLGR1, namely the human Usher syndrome type 2C and epilepsy.

2. Material and Methods

2.1 Animals

All experiments were performed in compliance with guidelines established by the Association for Research in Vision and Ophthalmology. Mice were kept under 12/12 hours light/dark cycles, food and water *ad libitum*. *Vlgr1/del7TM* mice carry a premature STOP codon at the exon 82 of *Vlgr1* which leads to the deletion of the entire 7TM domain and only the expression

of the extracellular domain ²⁷. The breeding background of *Vlgr1*^{del7}TM mice was the C57BL/6 strain which were also used as wild type (WT) controls.

2.2 Antibodies

Primary antibodies used in this study were the following: rabbit anti-p62 (Proteintech, 18420-1-AP), rabbit anti-LC3 (Proteintech, 14600-1-AP), mouse anti GAPDH (Abcam, ab9484), mouse anti-actin (Thermo Fisher Scientific, MA5-11869). Secondary antibodies used in this study were conjugated to Alexa 488, Alexa 555, or Alexa568, purchased from Invitrogen or Rockland Immunochemicals. Nuclear DNA was stained with DAPI (4',6-diamidino-2-phenylindole) (1 mg/ml, diluted 1:12000) (Sigma-Aldrich).

2.3 Cell culture

hTERT-RPE1 cells were cultured in Dulbecco's Modified Eagle Medium/Nutrient Mixture F-12 (Thermo Fisher Scientific) containing 10% heat-inactivated fetal calf serum (FCS). Cells were transfected with GeneJuice® (Merck Millipore) according to the manufacturer's instructions.

2.4 Human primary fibroblast cultures

Healthy dermal primary fibroblast lines were expanded from skin biopsies of human subjects (ethics vote: Landesärztekammer Rheinland-Palatinate to KNW). Primary fibroblast lines were mycoplasma negative and cultured in DMEM, 10% FCS and 1% penicillin-streptomycin at 37°C and 5% CO₂. USH2C *VLGR1/ADGRV1* R2959* patient-derived fibroblasts were a kind gift from Dr Erwin van Wijk (Radboud University Medical Center, Nijmegen) and were derived from skin biopsies of a 57-year-old male USH2C patient who carries a nonsense mutation in the *VLGR1/ADGRV1* gene (g.[90006848C>T])²⁸.

2.5 DNA constructs

VLGR1_CTF (Uniprot ID Q8WXG9-1, aa 5891-6306) sequence was used for VLGR1 constructs. For tandem affinity purifications, Strep II-FLAG (SF)-tagged human VLGR1_CTF was used. The SF-tag was N-terminally and C-terminally fused to VLGR1_CTF.

2.6 Tandem affinity purification (TAP) and mass spectrometry

Tandem affinity purification and mass spectrometry analysis were performed as previously described^{5,15,29}. The constructs illustrated in Figure 1A were expressed in HEK293T cells. After 48 h incubation, cells were lysed, cleared by centrifugation and supernatants were subsequently purified by using Strep-Tactin® Superflow® beads (IBA) and anti-Flag M2 agarose beads (Merck). Precipitation of eluates was performed with Methanol-chloroform. These eluates were

then used for liquid chromatography coupled with tandem mass spectrometry (LC-MS/MS). To validate the MS/MS-based peptide and polypeptide identifications, raw MS spectra were searched against the human SwissProt database using Mascot. The obtained results were additionally verified by Scaffold (version 4.02.01, Proteome Software Inc). Results were compared to mock-transfected cells and common RAF1 control TAPs. Proteins evident in mock and RAF1 Taps were excluded from the analysis. VLGR1 preys were used as input for the Cytoscape plugins STRING and ClueGO according to their gene names based on HGNC. Gene Ontology (GO) term enrichment analysis was performed by ClueGO v2.3.3.

2.7 siRNA-mediated knockdown in hTERT-RPE1 cells

Human hTERT-RPE1 cells were transfected with siRNAs specific for human *VLGR1* (L-005656-00-0005) and non-targeting control (NTC) siRNAs (D-001810-10-05), previously validated¹³. siRNAs were transfected using Lipofectamine RNAiMAX (Invitrogen) according to the manufacturer's instructions.

2.8 Arrest of autophagy in hTERT-RPE1 cells and primary dermal fibroblasts

To induce starvation of hTERT-RPE1 and primary dermal fibroblasts normal growth media were changed to Earle's Balanced Salt Solution (EBSS) and control cells were continually kept in normal growth media for 2 h. To arrest of autophagy cells were additionally treated with 5 μ M Bafilomycin A1 (BA1) (Sigma-Aldrich). Subsequently cells process

2.9 Immunocytochemistry

Cells were cultured on glass coverslips and fixed with 4% paraformaldehyde for 10 min at room temperature (RT), washed with PBS three times, permeabilized with PBST (0.2% Triton-X100 (Roth)) 10 min at RT, washed once with PBS and blocked with 0.1% ovalbumin, 0.5% fish gelatin in PBS for 1 h at RT. Primary antibodies were incubated overnight at 4°C, followed by washing three times with PBS and secondary antibody incubations for 1 h at RT. After another three times of washing with PBS, cells were mounted with Mowiol 4.88 (Hoechst) and analyzed with a Leica DM6000B microscope (Leica). Fiji/ImageJ software (NIH) was used for image processing and quantifications. For statistical analysis, R-Studio was used³⁰.

2.10 Data processing

For the analysis of p62/SQSTM1 positive dots during immunostaining, quantification was done using the Fiji/ImageJ software (<https://fiji.sc>). Images were loaded into Fiji using the Bio-Formats plugin. Cells were manually encircled, and the threshold was adjusted to Intermodes.

The selected cells were analyzed for dot number with the Fiji function analyze particles. The numbers were summarized in Excel and an average number per cell was calculated.

2.11 Western blot analyses

Protein lysates were prepared using Triton-X-100 lysis buffer (50 mM Tris/HCl, 150 mM NaCl, 0.5% Triton-X-100, pH 7.4) containing complete protease inhibitor cocktail (04693132001, Roche Diagnostics) and sonicated. Protein content was quantified using a BCA protein assay (Merck Millipore) and subjected to SDS-PAGE. The proteins were transferred to a polyvinylidene difluoride (PVDF) membrane (Merck Millipore). After blotting, membranes were blocked in AppliChem blocking reagent (AppliChem) for 1 h and subsequently incubated with primary antibodies overnight at 4°C followed by appropriate secondary antibodies Alexa Flour 680 (Invitrogen) or IR Dye 800 (Rockland). Scans of the blots were made employing the Odyssey infrared imaging system (LI-COR Biosciences). For densitometry analysis, the LI-COR software Empiria Studio was used, and for statistical analysis, R-Studio was applied³⁰.

2.12 RNA isolation and transcriptome sequencing

Adult (pn 40) WT and *Vlgr1/del7TM* mice were euthanized using cervical dislocation. Directly following the skull was opened and the brain was dissected to obtain the hippocampus, the cerebellum, and the cortex. The retina was extracted from the eyes. Tissues were flash-frozen using liquid nitrogen. Tissues were homogenized in RNeasy lysis buffer using 27 gauge needles, following RNA was isolated according to the instructions of the Qiagen RNeasy Mini Kit. RNA quality was determined using a Nanodrop (Thermo Fisher Scientific), and RNA was subsequently stored at -80°C. Whole transcriptome sequencing was performed by the company Novogene. mRNA sequencing was performed using the Illumina platform. Pair end reads were mapped and quantified. Following, differential gene expression analysis and Gene Ontology (GO) enrichment analysis was performed (<https://en.novogene.com/services/research-services/transcriptome-sequencing/mrna-sequencing/>).

2.13 Policy for experimental and clinical studies

The study was conducted in accordance with the Basic & Clinical Pharmacology & Toxicology policy for experimental and clinical studies³¹.

3. Results

3.1 Analysis of TAP data sets identified interactions of VLGR1/ADGRV1 with core components of the autophagy process.

We have recently identified more than 1000 putative interacting partners of VLGR1 in tandem purifications (TAPs) with VLGR1_ICD, VLGR1_CTFs, and full-length VLGR1a as baits ⁵. GO term analysis of the TAP datasets using the Cytoscape plugin ClueGO (accessed September 28, 2022) revealed numerous associations of VLGR1 with autophagy in the different GO categories (Figure 1C-G). In TAPs with full-length VLGR1a and both, the N- or C-terminal SF-tagged VLGR1_CTFs, 53 proteins associated with autophagy were enriched (Table 1). In contrast, no proteins associated with autophagy were found in the VLGR1_ICD TAP.

We used the GO aspect “Biological Process” and categorized the TAP hits into the three GO terms “autophagy”, “macroautophagy”, and “mitophagy”. For the term “autophagy”, we found 48 proteins in total for VLGR1a for both VLGR1_CTF. Approx. 80% of the proteins identified for the two VLGR1_CTFs were overlapping. For all three constructs together, the overlap was 40% of the identified proteins. Interestingly the autophagy core component ATG9a is only associated with SF-VLGR1_CTF, similarly, AMBRA1 is only present in the VLGR1a TAP. A STRING network analysis revealed multiple interactions between prey proteins of the GO term “autophagy” (Figure 1C).

For the downstream GO terms “macroautophagy” and “mitophagy” we identified 35 proteins and 6 proteins, respectively (Figure 1D, E; right hand). For both terms, the biggest overlap was between all three baits and between the two CTFs. Again, autophagy core components were identified for VLGR1a (AMBRA1, PIK3R2) and the two VLGR1_CTFs (TMEM59). In the String network, several of the identified proteins cluster in specific subgroups (Figure 1D, E; left hand).

In the category *Cellular component* TAP hits could be categorized by ClueGO into the three GO terms “autophagosome” and “lysosome”, 8 proteins and 26 proteins, respectively (Figure 1F, G). Most of the proteins identified for “autophagosomes” were present in TAP data of full-length VLGR1a and both VLGR1_CTFs or were found in TAPs of both VLGR1_CTFs. For “lysosome”, only in the two CTF TAP data sets, associated proteins were identified. As in the category *Biological process*, we found in the category *Cellular component* the autophagy core components ATG9a, AMBRA1, STX17, TM9SF1, and PIK3R4. The String network for the “autophagosome” clustered into two groups, autophagy core components and the group of ubiquitins and ubiquitin-associated proteins (Figure 1F). Several of the proteins associated with lysosomes, group together in the String network (Figure 1G).

We confirmed the GO term analyses by comparison with the data sets recently published gene toolbox for monitoring autophagy transcription ²¹. All prey proteins identified in our VLGR1-TAP categorized in the autophagy-related GO terms in the categories *Biological*

process and *Cellular component* were found in the subcategories of the autophagy process defined in this autophagy toolbox (Figure 1 H).

In summary, the identification of proteins participating in the autophagy process as potential interaction partners of VLGR1 indicated a close association of VLGR1 with autophagy.

3.2 RNA sequencing of *Vlgr1*-deficient retinæ revealed multiple associations of VLGR1 to autophagy molecules

We next explored whether there were any differences in the expression of genes related to autophagy in the absence of regular *VLGR1* expression. To this end, we performed genome-wide mRNA sequencing of retinas from *Vlgr1*-mutated and deficient *Vlgr1/del7TM* mice compared to wild-type retinæ samples. Total RNA was extracted from three biological replicates each of adult (pn 40) wild type and *Vlgr1/del7TM* retinæ, followed by RNA sequencing of the samples using the Illumina platform. Pair end reads were mapped and quantified, followed by differential gene expression analysis and Gene Ontology (GO) enrichment analysis (accessed on 18.05.2022). In total 2,824 genes were differentially expressed in *Vlgr1/del7TM* retinæ compared to WT retinæ: 1,671 of those were upregulated, and 1,153 were downregulated (Table S1, S2).

Using the recently defined autophagy gene toolbox with defined categories of functional classes²¹ we identified 30 genes that were differentially expressed in *Vlgr1/del7TM* retinæ (Figure 2A, B). From these genes 7 genes were down-regulated and 23 up-regulated with simple to high significance in *Vlgr1/del7TM* retinæ. The downregulated genes could be categorized into the terms “mTOR and upstream pathways”, “autophagy core machinery”, and “autophagy regulators” (Figure 2B). Among those genes, *Rps6kb2* and *Slc38a9* are core components of the mTOR pathway, and *Nek9* and *Stk38* play important roles in selective and chaperone-mediated autophagy.

The downregulated genes spanned all categories, except for docking and fusion. For example, a group of ATPase genes (*Atp6ap2*, *Atp6v1b2*, *Atp6v1c1*), important for lysosome function, four activating transcription factors (*Atf2*, *Atf3*, *Atf4*, *Atf5*), which regulate autophagy in response to various stresses, and the important autophagy adapter protein *p62/sqstm1* were downregulated in *Vlgr1* deficient retinæ. Additional GO-Term analysis revealed that genes differentially expressed in the *Vlgr1/del7TM* retinæ associate with the following *Biological process* subcategories: 58 genes with “autophagy”, 33 genes with “macroautophagy”, 6 genes with “mitoautophagy”, and 36 genes with “regulation of autophagy” (Figure 2C).

Taken together, the deficiency of *Vlgr1* leads to the dysregulation of the expression of genes related to autophagy in the mouse retina. Furthermore, this confirms the close relation of VLGR1 to autophagy processes indicated by the potential interacting proteins of the VLGR1 protein identified by TAP-based affinity proteomics.

3.3 Depletion of *VLGR1* increases autophagy in hTERT-RPE1 cells

Next, we investigated the consequences of *VLGR1* deficiency on autophagy. For this, we depleted *VLGR1* in hTERT-RPE1 cells by siRNA-mediated knockdown and then activated autophagy by starvation. To evaluate the levels of the key autophagy markers LC3 and p62 we arrested the autophagic flux. Autophagic flux is the formation of autophagosomes at compartments like the MAMs and then eventually the fusion of these with lysosomes. In the formed autolysosomes proteins or organelles get degraded. To establish an autophagy arrest, we blocked the fusion of autophagosomes with lysosomes using Bafilomycin A1 to prevent lysosome acidification and protein degradation (Figure 3).

In Western blots of cell lysates, we determined the protein content of the autophagy marker LC3, which is converted from the cytoplasmic form LC3I to the autophagosome membrane-bound form LC3II during autophagy (Figure 3A). The increased ratio of LC3II/LC3I observed in starved cells compared to unstarved cells confirmed that starvation increases autophagy in hTERT-RPE1 cells (Figure 3 A, B, D). In addition, siRNA-mediated knockdown of VLGR1 increased the LC3II/LC3I ratio in hTERT-RPE1 cells when compared to non-targeting control (NTC) siRNA-treated cells (Figure 3 A, C, E).

In the cytoplasm, autophagic cargos (liquid droplets, damaged organelles and aggregated proteins) are tagged with ubiquitin chains to which the autophagy adaptor protein p62 can bind³². This allows p62 antibodies to serve as a common marker for autophagosomes in immunocytochemistry. Immunocytochemical staining revealed an accumulation of anti-p62-positive dot-like structures representing autophagosomes in starved, Bafilomycin A1-treated hTERT-RPE1 cells (Figure 3F). Quantification revealed a highly significant increase of anti-p62-positive autophagosomes after *VLGR1*-depletion when compared to the NTC-treated hTERT-RPE1 cells (Figure 3 G).

Our combined results using the autophagy marker LC3 or p62 showed significant increases in autophagy in hTERT-RPE1 cells depleted for *VLGR1*.

3.4 Autophagic activity is greatly increased in USH2C patient-derived dermal fibroblasts

Next, we analysed the activity of autophagy in dermal fibroblasts derived from skin biopsies of a clinically characterized USH2C patient with a pathogenic mutation in *VLGR1/ADGRV1*. The *VLGR1/ADGRV1*^{Arg2959*} nonsense mutation leads to premature termination of translation and should result in the expression of a very truncated non-functional VLGR1 protein or due to nonsense-mediated mRNA decay no VLGR1 protein expression at all.

We starved USH2C fibroblast and control fibroblasts derived from a healthy individual, treated both with Bafilomycin A1 and analysed the autophagy activity in Western blots and by immunocytochemistry (Figure 4A). The LC3II/LC3I ratio of protein levels determined in Western blots revealed a significant increase of autophagy in USH2C fibroblasts when compared to control fibroblasts derived from a healthy individual (Figure 4A-E). Immunohistochemical analysis showed a significant increase of anti-p62-positive autophagosomes in USH2C patient-derived fibroblast compared to healthy controls (Figure 4F, G).

Taken together, our complementary assays revealed that the autophagy activity is significantly increased in both the knockdown of *VLGR1* in hTERT-RPE1 cells and the absence of functional VLGR1 protein in USH2C patient-derived fibroblast.

4. Discussion

In the present study, we identified close associations of the adhesion GPCR *VLGR1/ADGRV1* with autophagy (macro-autophagy), a conserved catabolic process of the cell proceeding the clearance of dysfunctional proteins, protein aggregates, and organelles by “self-digestion”^{24,33}. Autophagy is highly dynamic, characterized by sequential steps of the formation of autophagosomes from the phagophore and the fusion with lysosomes leading to digestive autolysosomes^{17,21}.

Applying an affinity capture approach based on tandem affinity purifications (TAPs), we identified several autophagy core proteins as putative interaction partners of VLGR1 (Figure 1). The absence of any autophagy-related proteins in TAPs with the cytoplasmic C-terminal domain (ICD) and the high number of preys found in both VLGR1 CTFs indicate that VLGR1 likely interacts with components of the autophagy machinery through the seven transmembrane membrane domain of VLGR1. The recently published autophagy monitoring toolbox²¹, allowed us to assign these autophagy proteins to diverse, almost all stages of the autophagy

process from the initial phagophore to the digestive autolysosome, suggesting that VLGR1 is present almost throughout the entire autophagy process. One explanation for this is that VLGR1 polypeptides tagged and overexpressed for TAPs are recognized as defective in the cell and degraded via autophagy, thereby interacting with the autophagy molecules. This should then be true for other adhesion GPCRs that we have recently studied by TAPs¹². However, we did not identify any autophagy molecules or much less prey in TAPs with adhesion GPCRs other than VLGR1. The potential physical interaction with key autophagy proteins may therefore indicate a role of VLGR1 in the control of the autophagy process. This is supported by our finding that the deficiency of VLGR1 in the *Vlgr1/del7TM* mouse model leads to alterations in the expression of numerous autophagy-related genes. Elevated autophagy activity observed after silencing of *VLGR1* in hTERT-RPE1 cells and VLGR1-deficient fibroblasts derived from USH1C patients further confirms a regulatory role of VLGR1 in the autophagy process, which is also in line with the putative interaction of VLGR1 with KEAP1 categorized as “regulation of autophagy”²¹.

The core autophagy proteins ATG9a, AMBRA1, RAB1A, or PIK3R4, found as prey in VLGR1 TAPs, are known to be essential in the initiation steps of the autophagy which may be indicative for VLGR1’s participation there³⁴⁻³⁷. The role of VLGR1 in the initiation of the autophagy processes is also consistent with the localization of VLGR1 as a specific site of the ER membrane, the mitochondria-associated ER membranes (MAMs) as we have recently demonstrated¹⁵. Indeed, MAMs have been identified as a compartment of initiation for autophagy at which autophagosome formation starts¹⁶. The absence of VLGR1 resulted in a disturbance in the MAM architecture and the dysregulation of the Ca²⁺ transient from ER to mitochondria¹⁵. The disruption of Ca²⁺ signalling between the ER and mitochondria and the resulting imbalance of Ca²⁺ homeostasis induces mitophagy^{38,39}, a specific form of autophagy which selectively removes defective mitochondria²². We additionally identified several proteins related to mitophagy, as potential interactors of VLGR1 (see Figure 1E, H) supporting the association of VLGR1 with this form of autophagy.

Another set of proteins found in VLGR1 TAPs was grouped into categories related to the process of autophagosome-lysosome fusion and lysosomal digestion. Deficiencies in those proteins, namely MCL1, VCP, NPC1, STX17, or LAMP2 lead to the increase of autophagic fluxes or extensive accumulation of autophagic aggregates⁴⁰⁻⁴⁴. This is exactly what we observed in the present study in the VLGR1 deficient hTERT-RPE1 cells and USH2C patient-derived fibroblasts evidencing a potential role of VLGR1 in the conversion of the autophagosome to the digestive autolysosome.

Multiple signals downstream of GPCRs regulate autophagy⁴⁵. A variety of GPCRs, such as the muscarinic, the glucagon-like peptide-1 (GLP-1), the β -adrenergic, or the purinergic GPCRs couple through $G\alpha_i$, $G\alpha_s$ or $G\alpha_q$ and the liberation of $G\beta\gamma$ mostly promote autophagy via second messenger cascades, e.g. cAMP or Ca^{2+} . As with other adhesion GPCRs, self-cleavage of VLGR1 at the GPS in the GAIN domain results in the separation of the extracellular N-terminal fragment (NTF) and the C-terminal fragment (CTF). This leads also to the activation of the receptor by binding of a tethered agonist, a short peptide of the very N-terminal part of the CTF called “Stachel” (Figure 1A), to the exoplasmic face of the receptor^{5,46}. There is growing evidence that the resulting conformation change in the VLGR1 also leads to the switch in the G protein coupling from $G\alpha_s$ constitutively coupled to the full-length uncleaved VLGR1 to $G\alpha_i$ -mediated signalling by the “activated” VLGR1-CTF^{5,47,48}. It has been previously shown that both, $G\alpha_s$ - and $G\alpha_i$ signalling cascades can context-dependently regulate autophagy⁴⁵. $G\alpha_s$ interacts with the adenylate cyclase and cAMP to induce autophagy whereas $G\alpha_i$ can activate autophagy through the LKB1/AMPK axis^{49,50}. Both downstream pathways have been linked to VLGR1⁵.

We have recently shown that VLGR1 functions as a metabotropic mechanoreceptor in focal adhesions by shear stress experiments¹³. Recent findings indicate that the sensing of mechanical stresses also contributes directly to the activation of autophagy²⁶. By physical interaction of core proteins of both autophagy and focal adhesion, paxillin promotes the disassembly of focal adhesions and cell motility⁵¹. As we have recently demonstrated VLGR1 is also key in the regulation of focal adhesion dynamics and cell migration^{13,14}. Taken together, our data provide evidence that VLGR1 regulates the two interrelated processes of autophagy and cell migration by sensing mechanical signals at focal adhesions.

Mutations in *VLGR1/ADGRV1* are the cause of Usher syndrome type 2, characterized by congenital sensorineural hearing loss and retinitis pigmentosa (RP)⁷. In the present study, we demonstrated that in cellular models, namely after *VLGR1/ADGRV1* silencing in hTERT-RPE1 cells and fibroblasts fromUSH1C patients, autophagy activity is significantly increased. This was confirmed by our transcriptome data obtained from the retina of the *Vlgr1/del7TM* mouse model demonstrating the upregulation of key autophagy genes compared to the wild type. Among these genes, *Nek9* was upregulated in the *Vlgr1*-deficient mouse retina. The encoded NIMA-related kinase 9 (NEK9) is a selective autophagy adaptor essential for the formation of primary cilia⁵². We have recently that VLGR1 participates also in ciliogenesis⁵ and a mutual pathway between NEK9 and VLGR1, related autophagy for the promotion of ciliogenesis seems reasonable.

In the sensory cells of the eye and ear, USH type 2 proteins physically interact in membrane-membrane adhesion complexes and therefore defects in both molecules are thought to result in the same pathomechanisms leading to the disease ^{7,53,54}. Indeed, an increase in autophagy has been recently reported in a *USH2A* zebrafish model associated with retinal degeneration ⁵⁵. Because the USH2 proteins VLGR1 and USH2A physically interact in membrane-membrane adhesion complexes of photoreceptor and hair cells, the sensory cells affected by USH disease in the eye and ear, defects in both molecules most likely result in the same pathomechanisms leading to USH. This finding is confirmed by our transcriptome data obtained from the retina of the *Vlgr1/del7TM* mouse model, which demonstrates the upregulation of key autophagy genes compared to the wild type.

Besides USH2C, defects, namely haploinsufficiency of *VLGR1/ADGRV1* can also lead to the development of epilepsy in humans ^{9,56} and audiogenic epilepsy in mice ². There is increasing evidence that alterations in autophagy are present in epileptogenesis, leading to imbalanced excitatory-inhibitory neurotransmission and epilepsy-induced neuronal damage ^{57,58}. It is notable, the application of the inhibitor rapamycin of the mTOR pathway, which induces autophagy reduces the seizure frequency *in vivo*. Interestingly, RNAseq data of the retina of *Vlgr1/del7TM* mouse, a validated audiogenic seizure model, indicated differential expression, mainly up-regulation, of genes related to the mTOR pathway (Figure 2). A link of VLGR1 to the mTOR pathway is further supported by the identifications of mTOR pathway components as potential interacting partners of VLGR1 by the present TAPs (Figure 1). Collectively, *VLGR1/ADGRV1*-associated epilepsy may be associated with disruption of the mTOR pathway and altered autophagy, opening possible treatment options with rapamycin.

5. Conclusions

In conclusion, we provide evidence that the USH2C protein VLGR1 interacts with autophagy core proteins imitating autophagy and with molecules related to autolysosome formation, indicating a close association of VLGR1 with autophagy. In the absence of VLGR1 autophagy activities increases and leads to differential expression of genes related to autophagy. Our findings support the role of VLGR1 in the control of autophagy in a multifaceted way at internal membranes of the ER, mitochondria and focal adhesions and provide evidence of the role of autophagy in the pathophysiology of VLGR1-related diseases, such as human Usher syndrome and epilepsy.

Author Contributions: J.L. conducted the majority of the experiments, analysis of data, and figure preparation. B.E.G. helped isolate mice retinæ for RNA sequencing. J.K. performed the

TAP assays and assisted during data processing. U.W. and J.L. designed the studies. U.W. and J.L. wrote the manuscript. All authors have read and agreed to the published version of the manuscript.

Acknowledgements: We thank Dr Barbara Knapp for providing data on initial TAPs and Drs Erwin van Wijk and Kerstin Nagel-Wolfrum for kindly providing dermal fibroblasts of a USH2C patient and healthy individual, respectively. We further thank Ulrike Maas for her skilful technical support in biochemistry.

Funding: This work was supported by grants to U.W. from The German Research Council DFG FOR 2149 Elucidation of Adhesion-GPCR Signaling, project number 246212759 and The Foundation Fighting Blindness (FFB) PPA-0717-0719-RAD.

Institutional Review Board Statement: The use of mice in research was approved by the German regulation authority for the use of animals in research, the district administration Mainz-Bingen, 8341a/177-5865-§11 ZVTE, 30.04.2014.

Conflict of interest: The authors declare no conflict of interest.

References

1. McGee JA, Goodyear RJ, McMillan DR, et al. The very large G-protein-coupled receptor VLGR1: A component of the ankle link complex required for the normal development of auditory hair bundles. *Journal of Neuroscience*. 2006;26(24):6543-6553. doi:10.1523/JNEUROSCI.0693-06.2006
2. McMillan DR, White PC. *Studies On The Very Large G Protein-Coupled Receptor: From Initial Discovery to Determining Its Role in Sensorineural Deafness in Higher Animals.*; 2010.
3. Liebscher I, Schöneberg T. Tethered Agonism: A Common Activation Mechanism of Adhesion GPCRs. In: ; 2016:111-125. doi:10.1007/978-3-319-41523-9_6
4. Liebscher I, Schöneberg T, Thor D. Stachel-mediated activation of adhesion G protein-coupled receptors: insights from cryo-EM studies. *Signal Transduct Target Ther*. 2022;7(1). doi:10.1038/s41392-022-01083-y
5. Knapp B, Roedig J, Roedig H, et al. Affinity Proteomics Identifies Interaction Partners and Defines Novel Insights into the Function of the Adhesion GPCR VLGR1/ADGRV1. *Molecules*. 2022;27(10). doi:10.3390/molecules27103108
6. Reiners J, Nagel-Wolfrum K, Jürgens K, Märker T, Wolfrum U. Molecular basis of human Usher syndrome: Deciphering the meshes of the Usher protein network provides insights into the pathomechanisms of the Usher disease. *Exp Eye Res*. 2006;83(1):97-119. doi:10.1016/j.exer.2005.11.010

7. Fuster-García C, García-Bohórquez B, Rodríguez-Muñoz A, et al. Usher syndrome: Genetics of a human ciliopathy. *Int J Mol Sci.* 2021;22(13). doi:10.3390/ijms22136723
8. Myers KA, Nasioulas S, Boys A, et al. ADGRV1 is implicated in myoclonic epilepsy. *Epilepsia.* 2018;59(2):381-388. doi:10.1111/epi.13980
9. Dahawi M, Elmagzoub MS, A. Ahmed E, et al. Involvement of ADGRV1 Gene in Familial Forms of Genetic Generalized Epilepsy. *Front Neurol.* 2021;12(October):1-10. doi:10.3389/fneur.2021.738272
10. Michel V, Goodyear RJ, Weil D, et al. Cadherin 23 is a component of the transient lateral links in the developing hair bundles of cochlear sensory cells. *Dev Biol.* 2005;280(2):281-294. doi:10.1016/j.ydbio.2005.01.014
11. Maerker T, van Wijk E, Overlack N, et al. A novel Usher protein network at the periciliary reloading point between molecular transport machineries in vertebrate photoreceptor cells. *Hum Mol Genet.* 2008;17(1):71-86. doi:10.1093/hmg/ddm285
12. Knapp B, Roedig J, Boldt K, et al. Affinity proteomics identifies novel functional modules related to adhesion GPCRs. In: *Annals of the New York Academy of Sciences.* Vol 1456. Blackwell Publishing Inc.; 2019:144-167. doi:10.1111/nyas.14220
13. Kusuluri DK, Güler BE, Knapp B, et al. Adhesion G protein-coupled receptor VLGR1/ADGRV1 regulates cell spreading and migration by mechanosensing at focal adhesions. *iScience.* 2021;24(4). doi:10.1016/j.isci.2021.102283
14. Güler BE, Linnert J, Wolfrum U. *The Adhesion GPCR VLGR1/ADGRV1 Regulates Focal Adhesion Turnover by Controlling Their Assembly.*
15. Krzysko J, Maciag F, Mertens A, et al. The Adhesion GPCR VLGR1/ADGRV1 Regulates the Ca²⁺ Homeostasis at Mitochondria-Associated ER Membranes. *Cells.* 2022;11(18). doi:10.3390/cells11182790
16. Hamasaki M, Furuta N, Matsuda A, et al. Autophagosomes form at ER-mitochondria contact sites. *Nature.* 2013;495(7441):389-393. doi:10.1038/nature11910
17. Mizushima N, Komatsu M. Autophagy: Renovation of cells and tissues. *Cell.* 2011;147(4):728-741. doi:10.1016/j.cell.2011.10.026
18. Tanida I. Autophagy basics. *Microbiol Immunol.* 2011;55(1):1-11. doi:10.1111/j.1348-0421.2010.00271.x
19. Deretic V, Saitoh T, Akira S. Autophagy in infection, inflammation and immunity. *Nat Rev Immunol.* 2013;13(10):722-737. doi:10.1038/nri3532
20. Wang CW, Klionsky DJ. *The Molecular Mechanism of Autophagy.*; 2003.
21. Bordi M, de Cegli R, Testa B, Nixon RA, Ballabio A, Cecconi F. A gene toolbox for monitoring autophagy transcription. *Cell Death Dis.* 2021;12(11):1-7. doi:10.1038/s41419-021-04121-9
22. Ding WX, Yin XM. Mitophagy: Mechanisms, pathophysiological roles, and analysis. *Biol Chem.* 2012;393(7):547-564. doi:10.1515/hsz-2012-0119

23. Liang JR, Lingeman E, Luong T, et al. A Genome-wide ER-phagy Screen Highlights Key Roles of Mitochondrial Metabolism and ER-Resident UFMylation. *Cell*. 2020;180(6):1160-1177.e20. doi:10.1016/j.cell.2020.02.017
24. Vargas JNS, Hamasaki M, Kawabata T, Youle RJ, Yoshimori T. The mechanisms and roles of selective autophagy in mammals. *Nat Rev Mol Cell Biol*. Published online 2022. doi:10.1038/s41580-022-00542-2
25. Yao J, Qiu Y, Frontera E, et al. Inhibiting autophagy reduces retinal degeneration caused by protein misfolding. *Autophagy*. 2018;14(7):1226-1238. doi:10.1080/15548627.2018.1463121
26. Hernández-Cáceres MP, Munoz L, Pradenas JM, et al. Mechanobiology of Autophagy: The Unexplored Side of Cancer. *Front Oncol*. 2021;11(February):1-20. doi:10.3389/fonc.2021.632956
27. Sridhar S, Botbol Y, MacIain F, Cuervo AM. Autophagy and disease: Always two sides to a problem. *Journal of Pathology*. 2012;226(2):255-273. doi:10.1002/path.3025
28. Usher Syndrome Database. Accessed November 9, 2022. <https://databases.lovd.nl/shared/variants/GPR98/unique>
29. Boldt K, van Reeuwijk J, Lu Q, et al. An organelle-specific protein landscape identifies novel diseases and molecular mechanisms. *Nat Commun*. 2016;7. doi:10.1038/ncomms11491
30. RStudio Team. RStudio: Integrated Development Environment for R. Published online 2020.
31. Tveden-Nyborg P, Bergmann TK, Jessen N, Simonsen U, Lykkesfeldt J. BCPT policy for experimental and clinical studies. *Basic Clin Pharmacol Toxicol*. 2021;128(1):4-8. doi:10.1111/bcpt.13492
32. Kageyama S, Gudmundsson SR, Sou YS, et al. p62/SQSTM1-droplet serves as a platform for autophagosome formation and anti-oxidative stress response. *Nat Commun*. 2021;12(1). doi:10.1038/s41467-020-20185-1
33. Klionsky DJ, Abdel-Aziz AK, Abdelfatah S, et al. Guidelines for the use and interpretation of assays for monitoring autophagy (4th edition)1. *Autophagy*. 2021;17(1):1-382. doi:10.1080/15548627.2020.1797280
34. Young ARJ, Chan EYW, Hu XW, et al. Starvation and ULK1-dependent cycling of mammalian Atg9 between the TGN and endosomes. *J Cell Sci*. 2006;119(18):3888-3900. doi:10.1242/jcs.03172
35. Maria Fimia G, Stoykova A, Romagnoli A, et al. Ambra1 regulates autophagy and development of the nervous system. *Nature*. 2007;447(7148):1121-1125. doi:10.1038/nature05925
36. Ao X, Zou L, Wu Y. Regulation of autophagy by the Rab GTPase network. *Cell Death Differ*. 2014;21(3):348-358. doi:10.1038/cdd.2013.187
37. Jean S, Kiger AA. Classes of phosphoinositide 3-kinases at a glance. *J Cell Sci*. 2014;127(5):923-928. doi:10.1242/jcs.093773

38. Puri R, Cheng XT, Lin MY, Huang N, Sheng ZH. Mulf1 restrains Parkin-mediated mitophagy in mature neurons by maintaining ER-mitochondrial contacts. *Nat Commun.* 2019;10(1). doi:10.1038/s41467-019-11636-5
39. Zhang D, Wang F, Li P, Gao Y. Mitochondrial Ca²⁺ Homeostasis: Emerging Roles and Clinical Significance in Cardiac Remodeling. *Int J Mol Sci.* 2022;23(6). doi:10.3390/ijms23063025
40. Fortunato F, Bürgers H, Bergmann F, et al. Impaired Autolysosome Formation Correlates With Lamp-2 Depletion: Role of Apoptosis, Autophagy, and Necrosis in Pancreatitis. *Gastroenterology.* 2009;137(1). doi:10.1053/j.gastro.2009.04.003
41. Pacheco CD, Kunkel R, Lieberman AP. Autophagy in Niemann-Pick C disease is dependent upon Beclin-1 and responsive to lipid trafficking defects. *Hum Mol Genet.* 2007;16(12):1495-1503. doi:10.1093/hmg/ddm100
42. Hegedus K, Takats S, Kovacs AL, Juhasz G. Evolutionarily conserved role and physiological relevance of a STX17/Syx17 (syntaxin 17)-containing SNARE complex in autophagosome fusion with endosomes and lysosomes. *Autophagy.* 2013;9(10):1642-1646. doi:10.4161/auto.25684
43. Elgendy M, Ciro M, Abdel-Aziz AK, et al. Beclin 1 restrains tumorigenesis through Mcl-1 destabilization in an autophagy-independent reciprocal manner. *Nat Commun.* 2014;5. doi:10.1038/ncomms6637
44. Yeo BK, Hong CJ, Chung KM, et al. Valosin-containing protein is a key mediator between autophagic cell death and apoptosis in adult hippocampal neural stem cells following insulin withdrawal. *Mol Brain.* 2016;9(1). doi:10.1186/s13041-016-0212-8
45. Wauson EM, Dbouk HA, Ghosh AB, Cobb MH. G protein-coupled receptors and the regulation of autophagy. *Trends in Endocrinology and Metabolism.* 2014;25(5):274-282. doi:10.1016/j.tem.2014.03.006
46. Lala T, Hall RA. Adhesion G Protein-Coupled Receptors: Structure, Signaling, Physiology, And Pathophysiology. *Physiol Rev.* 2022;102(4):1587-1624. doi:10.1152/physrev.00027.2021
47. Shin D, Lin ST, Fu YH, Ptáček LJ. Very large G protein-coupled receptor 1 regulates myelin-associated glycoprotein via Gas/Gaq-mediated protein kinases A/C. *Proc Natl Acad Sci U S A.* 2013;110(47):19101-19106. doi:10.1073/pnas.1318501110
48. Hu QX, Dong JH, Du HB, et al. Constitutive Gai coupling activity of very large G protein-coupled receptor 1 (VLGR1) and its regulation by PDZD7 protein. *Journal of Biological Chemistry.* 2014;289(35):24215-24225. doi:10.1074/jbc.M114.549816
49. Akhshi T, Trimble WS. A non-canonical hedgehog pathway initiates ciliogenesis and autophagy. *Journal of Cell Biology.* 2021;220(1). doi:10.1083/jcb.202004179
50. Yin XM, Ding WX, Gao W. Autophagy in the liver. *Hepatology.* 2008;47(5):1773-1785. doi:10.1002/hep.22146
51. Sharifi MN, Mowers EE, Drake LE, et al. Autophagy Promotes Focal Adhesion Disassembly and Cell Motility of Metastatic Tumor Cells through the Direct

- Interaction of Paxillin with LC3. *Cell Rep.* 2016;15(8):1660-1672.
doi:10.1016/j.celrep.2016.04.065
52. Yamamoto Y, Chino H, Tsukamoto S, Ode KL, Ueda HR, Mizushima N. NEK9 regulates primary cilia formation by acting as a selective autophagy adaptor for MYH9/myosin IIA. *Nat Commun.* 2021;12(1). doi:10.1038/s41467-021-23599-7
 53. Mathur PD, Yang J. Usher syndrome and non-syndromic deafness: Functions of different whirlin isoforms in the cochlea, vestibular organs, and retina. *Hear Res.* 2019;375:14-24. doi:10.1016/j.heares.2019.02.007
 54. Wolfrum U. *Usher Syndrome : Pathogenesis, Diagnosis, and Therapy.*; 2011.
 55. Toms M, Dubis AM, de Vrieze E, et al. Clinical and preclinical therapeutic outcome metrics for USH2A-related disease. *Hum Mol Genet.* 2020;29(11):1882-1899. doi:10.1093/HMG/DDAA004
 56. Zhou P, Meng H, Liang X, et al. ADGRV1 Variants in Febrile Seizures/Epilepsy With Antecedent Febrile Seizures and Their Associations With Audio-Visual Abnormalities. *Front Mol Neurosci.* 2022;15. doi:10.3389/fnmol.2022.864074
 57. Giorgi FS, Biagioni F, Lenzi P, Frati A, Fornai F. The role of autophagy in epileptogenesis and in epilepsy-induced neuronal alterations. *J Neural Transm.* 2015;122(6):849-862. doi:10.1007/s00702-014-1312-1
 58. Limanaqi F, Biagioni F, Busceti CL, Fabrizi C, Frati A, Fornai F. MTOR-related cell-clearing systems in epileptic seizures, an update. *Int J Mol Sci.* 2020;21(5). doi:10.3390/ijms21051642
 59. Nozawa T, Minowa-Nozawa A, Aikawa C, Nakagawa I. The STX6-VTI1B-VAMP3 complex facilitates xenophagy by regulating the fusion between recycling endosomes and autophagosomes. *Autophagy.* 2017;13(1):57-69. doi:10.1080/15548627.2016.1241924
 60. Tumbarello DA, Waxse BJ, Arden SD, Bright NA, Kendrick-Jones J, Buss F. Autophagy receptors link myosin VI to autophagosomes to mediate Tom1-dependent autophagosome maturation and fusion with the lysosome. *Nat Cell Biol.* 2012;14(10):1024-1035. doi:10.1038/ncb2589
 61. Rogov V, Dötsch V, Johansen T, Kirkin V. Interactions between Autophagy Receptors and Ubiquitin-like Proteins Form the Molecular Basis for Selective Autophagy. *Mol Cell.* 2014;53(2):167-178. doi:10.1016/j.molcel.2013.12.014
 62. Yun Lee D, Arnott D, Brown EJ. Ubiquilin4 is an adaptor protein that recruits Ubiquilin1 to the autophagy machinery. *EMBO Rep.* 2013;14(4):373-381. doi:10.1038/embor.2013.22
 63. Lu Y, Zhang Z, Sun D, Sweeney ST, Gao FB. Syntaxin 13, a genetic modifier of mutant CHMP2B in frontotemporal dementia, is required for autophagosome maturation. *Mol Cell.* 2013;52(2):264-271. doi:10.1016/j.molcel.2013.08.041

64. Bonam SR, Ruff M, Muller S. HSPA8/HSC70 in immune disorders: A molecular rheostat that adjusts chaperone-mediated autophagy substrates. *Cells*. 2019;8(8). doi:10.3390/cells8080849
65. Fedeli C, Filadi R, Rossi A, Mammucari C, Pizzo P. PSEN2 (presenilin 2) mutants linked to familial Alzheimer disease impair autophagy by altering Ca²⁺ homeostasis. *Autophagy*. 2019;15(12):2044-2062. doi:10.1080/15548627.2019.1596489
66. di Lorenzo G, Iavarone F, Maddaluno M, Grumati P, Settembre C. RETREG3/FAM134C phosphorylation by CSNK2 regulates reticulophagy during starvation. *Autophagy Reports*. 2022;1(1):519-522. doi:10.1080/27694127.2022.2131212
67. Chino H, Hatta T, Natsume T, Mizushima N. Intrinsically Disordered Protein TEX264 Mediates ER-phagy. *Mol Cell*. 2019;74(5):909-921.e6. doi:10.1016/j.molcel.2019.03.033
68. Journo D, Mor A, Abeliovich H. Aup1-mediated regulation of Rtg3 during mitophagy. *Journal of Biological Chemistry*. 2009;284(51):35885-35895. doi:10.1074/jbc.M109.048140
69. Garg AD, Dudek AM, Ferreira GB, et al. ROS-induced autophagy in cancer cells assists in evasion from determinants of immunogenic cell death. *Autophagy*. 2013;9(9):1292-1307. doi:10.4161/auto.25399
70. Jiang Q, Li F, Shi K, et al. ATF4 activation by the p38MAPK-eIF4E axis mediates apoptosis and autophagy induced by selenite in Jurkat cells. *FEBS Lett*. 2013;587(15):2420-2429. doi:10.1016/j.febslet.2013.06.011
71. Molejon MI, Ropolo A, Re A lo, Boggio V, Vaccaro MI. The VMP1-Beclin 1 interaction regulates autophagy induction. *Sci Rep*. 2013;3. doi:10.1038/srep01055
72. Mingione A, Cas MD, Bonezzi F, et al. Inhibition of sphingolipid synthesis as a phenotype-modifying therapy in cystic fibrosis. *Cellular Physiology and Biochemistry*. 2020;54(1):110-125. doi:10.33594/000000208
73. Cao Y, Li R, Shen M, et al. DDRGK1, a crucial player of ufmylation system, is indispensable for autophagic degradation by regulating lysosomal function. *Cell Death Dis*. 2021;12(5). doi:10.1038/s41419-021-03694-9
74. Eskelinen EL. Roles of LAMP-1 and LAMP-2 in lysosome biogenesis and autophagy. *Mol Aspects Med*. 2006;27(5-6):495-502. doi:10.1016/j.mam.2006.08.005
75. Yim WWY, Mizushima N. Lysosome biology in autophagy. *Cell Discov*. 2020;6(1). doi:10.1038/s41421-020-0141-7
76. Wen H, Zhan L, Chen S, Long L, Xu E. Rab7 may be a novel therapeutic target for neurologic diseases as a key regulator in autophagy. *J Neurosci Res*. 2017;95(10):1993-2004. doi:10.1002/jnr.24034
77. Itakura E, Kishi-Itakura C, Mizushima N. The hairpin-type tail-anchored SNARE syntaxin 17 targets to autophagosomes for fusion with endosomes/lysosomes. *Cell*. 2012;151(6):1256-1269. doi:10.1016/j.cell.2012.11.001

78. Fader CM, Sánchez DG, Mestre MB, Colombo MI. TI-VAMP/VAMP7 and VAMP3/cellubrevin: two v-SNARE proteins involved in specific steps of the autophagy/multivesicular body pathways. *Biochim Biophys Acta Mol Cell Res*. 2009;1793(12):1901-1916. doi:10.1016/j.bbamcr.2009.09.011
79. Lefebvre V, Du Q, Baird S, et al. Genome-wide RNAi screen identifies ATPase inhibitory factor 1 (ATPIF1) as essential for PARK2 recruitment and mitophagy. *Autophagy*. 2013;9(11):1770-1779. doi:10.4161/auto.25413
80. Jiang W, Ogretmen B. Ceramide stress in survival versus lethal autophagy paradox Ceramide targets autophagosomes to mitochondria and induces lethal mitophagy. *Autophagy*. 2013;9(2):258-259. doi:10.4161/auto.22739
81. Bhujabal Z, Birgisdottir ÁB, Sjøttem E, et al. FKBP8 recruits LC3A to mediate Parkin-independent mitophagy. *EMBO Rep*. 2017;18(6):947-961. doi:10.15252/embr.201643147
82. Wei Y, Chiang WC, Sumpter R, Mishra P, Levine B. Prohibitin 2 Is an Inner Mitochondrial Membrane Mitophagy Receptor. *Cell*. 2017;168(1-2):224-238.e10. doi:10.1016/j.cell.2016.11.042
83. Tanaka A, Cleland MM, Xu S, et al. Proteasome and p97 mediate mitophagy and degradation of mitofusins induced by Parkin. *Journal of Cell Biology*. 2010;191(7):1367-1380. doi:10.1083/jcb.201007013
84. Geisler S, Holmström KM, Skujat D, et al. PINK1/Parkin-mediated mitophagy is dependent on VDAC1 and p62/SQSTM1. *Nat Cell Biol*. 2010;12(2):119-131. doi:10.1038/ncb2012
85. di Rita A, Peschiaroli A, D'Acunzo P, et al. HUWE1 E3 ligase promotes PINK1/PARKIN-independent mitophagy by regulating AMBRA1 activation via IKK α . *Nat Commun*. 2018;9(1). doi:10.1038/s41467-018-05722-3
86. Wu T, Li Y, Huang D, et al. Regulator of G-protein signaling 19 (RGS19) and its partner G α -inhibiting activity polypeptide 3 (GNAI3) are required for zVAD-induced autophagy and cell death in L929 cells. *PLoS One*. 2014;9(4). doi:10.1371/journal.pone.0094634
87. Tan VP, Miyamoto S. HK2/hexokinase-II integrates glycolysis and autophagy to confer cellular protection. *Autophagy*. 2015;11(6):963-964. doi:10.1080/15548627.2015.1042195
88. Huang H, Ouyang Q, Zhu M, Yu H, Mei K, Liu R. mTOR-mediated phosphorylation of VAMP8 and SCFD1 regulates autophagosome maturation. *Nat Commun*. 2021;12(1). doi:10.1038/s41467-021-26824-5
89. Merkulova M, Paunescu TG, Azroyan A, Marshansky V, Breton S, Brown D. Mapping the H⁺ (V)-ATPase interactome: Identification of proteins involved in trafficking, folding, assembly and phosphorylation. *Sci Rep*. 2015;5. doi:10.1038/srep14827
90. Castellano BM, Thelen AM, Moldavski O, et al. Lysosomal cholesterol activates mTORC1 via an SLC38A9-Niemann-Pick C1 signaling complex. <https://www.science.org>

91. Behl C. BAG3 and friends: Co-chaperones in selective autophagy during aging and disease. *Autophagy*. 2011;7(7):795-798. doi:10.4161/auto.7.7.15844
92. Wang CH, Kao CH, Chen YF, Wei YH, Tsai TF. Cisd2 mediates lifespan: Is there an interconnection among Ca²⁺ homeostasis, autophagy, and lifespan? In: *Free Radical Research*. Vol 48. Informa Healthcare; 2014:1109-1114. doi:10.3109/10715762.2014.936431
93. Wang F, Liao Y, Zhang M, et al. N6-methyladenosine demethyltransferase FTO-mediated autophagy in malignant development of oral squamous cell carcinoma. *Oncogene*. 2021;40(22):3885-3898. doi:10.1038/s41388-021-01820-7
94. Li Y, Zhao Y, Hu J, et al. A novel ER-localized transmembrane protein, EMC6, interacts with RAB5A and regulates cell Autophagy. *Autophagy*. 2013;9(2):150-163. doi:10.4161/auto.22742
95. Komatsu M, Kurokawa H, Waguri S, et al. The selective autophagy substrate p62 activates the stress responsive transcription factor Nrf2 through inactivation of Keap1. *Nat Cell Biol*. 2010;12(3):213-223. doi:10.1038/ncb2021
96. Thomas RL, Gustafsson ÅB. MCL1 is critical for mitochondrial function and autophagy in the heart. *Autophagy*. 2013;9(11):1902-1903. doi:10.4161/auto.26168
97. Zhang J, Zhang Y, Liu S, et al. Metadherin confers chemoresistance of cervical cancer cells by inducing autophagy and activating ERK/NF-κB pathway. *Tumor Biology*. 2013;34(4):2433-2440. doi:10.1007/s13277-013-0794-z
98. Ghavami S, Eshragi M, Ande SR, et al. S100A8/A9 induces autophagy and apoptosis via ROS-mediated cross-talk between mitochondria and lysosomes that involves BNIP3. *Cell Res*. 2010;20(3):314-331. doi:10.1038/cr.2009.129
99. Miao G, Zhang Y, Chen D, Zhang H. The ER-Localized Transmembrane Protein TMEM39A/SUSR2 Regulates Autophagy by Controlling the Trafficking of the PtdIns(4)P Phosphatase SAC1. *Mol Cell*. 2020;77(3):618-632.e5. doi:10.1016/j.molcel.2019.10.035
100. Moretti F, Bergman P, Dodgson S, et al. TMEM 41B is a novel regulator of autophagy and lipid mobilization . *EMBO Rep*. 2018;19(9). doi:10.15252/embr.201845889
101. Boada-Romero E, Letek M, Fleischer A, Pallauf K, Ramón-Barros C, Pimentel-Muñoz FX. TMEM59 defines a novel ATG16L1-binding motif that promotes local activation of LC3. *EMBO Journal*. 2013;32(4):566-582. doi:10.1038/emboj.2013.8

Figure legends

Figure 1. GO term analysis of TAP data from the adhesion GPCR VLGR1. (A) VLGR1 isoform structure for VLGR1a and VLGR1b. (B) Illustration of VLGR1 baits used for tandem affinity purifications (TAPs): VLGR1a, the C-terminal fragment (CTF), or the intracellular domain (ICD) of VLGR1 were either N- or C-terminal tagged with Strep-FLAG. (C) Venn diagram of VLGR1 preys assigned to the GO term autophagy in the category Biological Process. The interaction of these prey is visualised in a STRING network. (D) Venn diagram and STRING network of VLGR1 prey assigned to the GO term macroautophagy. (E) Venn diagram and STRING network of VLGR1 prey associated with the GO term mitophagy. (F) Venn diagram and STRING network of VLGR1 prey associated with the GO term autophagosome in the category Cellular Component. (G) Venn diagram and STRING network of VLGR1 preys assigned to the GO term Lysosome. (H) Categorisation of the VLGR1 interactors associated with autophagy, identified by GO-term analysis, into subcategories of the autophagy process previously defined by Bordi and co-workers²¹.

Figure 2: Whole transcriptome sequencing of VLGR1 deficient mice retinae. (A) Heatmap of dysregulated genes associated with autophagy. Genes were chosen based on the autophagy gene toolbox created by Bordi and co-workers²¹. The dysregulation of these genes was highly significant. (B) Genes were again subcategorised into functional classes defined in the autophagy gene toolbox. (C) GO-term analysis of dysregulated genes. Venn-diagram shows results for the terms autophagy, macroautophagy, regulation of autophagy and mitophagy in the category biological process.

Figure 3: VLGR1 depletion increases the abundance of autophagy markers LC3 and p62 in RPE1 cells. (A) Western blot analysis of autophagy marker LC3 in VLGR1 and NTC-depleted RPE1 cells. Quantification (B, D) revealed an increase in the ratio of LC3II to LC3I already in starved control-depleted cells. (C, E) After VLGR1 depletion the ratio of LC3II to LC3I increased even greater when compared to the control. Ratios were normalized to loading control. (F) Immunolabelling of the autophagy marker p62 revealed an increase of p62 accumulations in VLGR1-depleted cells compared to control cells. Cells were treated for 2 h with 5 μ M Bafilomycin A1 and were cultured in EBSS to induce starvation. (G) Quantification confirmed that VLGR1-depleted cells show significantly more p62-positive accumulations than

control cells. Scale in F = 10 μ m. Statistical significance was determined by Mann–Whitney U test $*=p<0.05$, $**=p<0.01$, $***=p<0.005$.

Figure 4: VLGR1 deficiency in patient-derived fibroblasts increases autophagic activity.

(A) Western Blot analysis of patient-derived USH2C fibroblasts and healthy control cells. (B, D) Quantification revealed a significant increase in the ratio of LC3II to LC3I in starved healthy cells compared to unstarved cells. (C, E) VLGR1 deficient fibroblasts showed an even greater increase in the ratio of LC3II to LC3I compared to starved healthy cells. Ratios were normalized to loading control. (F) Immunolabeling of p62 revealed an increase of accumulations in patient-derived USH2C fibroblasts compared to healthy control cells. Cells were treated for 2h with 5 μ M Bafilomycin A1 and were cultured in EBSS to induce starvation. (G) Quantification revealed a significant increase of p62 accumulations in patient-derived USH2C cells compared to healthy control cells. Scale in F = 10 μ M Statistical significance was determined by Mann–Whitney U test $*=p<0.05$, $**=p<0.01$, $***=p<0.005$.

Tables

Table 1. Autophagy related proteins identified by VLGR1 TAPs

Gene	Protein	Autophagy related protein function	Reference
<i>RAB1A</i>	RAB1A, member RAS oncogene family	Autophagosome formation	36
<i>RAB8A</i>	RAB8A, member RAS oncogene family	Autophagosome formation	36
<i>STX12</i>	Syntaxin 12	Autophagosome maturation	59
<i>TOM1</i>	target of myb1 membrane trafficking protein	Autophagosome maturation	60
<i>UBQLN1</i>	Ubiquilin 1	Autophagosome maturation	61
<i>UBQLN2</i>	Ubiquilin 2	Autophagosome maturation	61
<i>UBQLN4</i>	Ubiquilin 4	Autophagosome maturation	62
<i>VTGA</i>	Vesicle transport through interaction with t-SNAREs 1A	Autophagosome maturation	63
<i>HSPA8</i>	Heat shock protein family A (Hsp70) member 8	Chaperone-mediated autophagy	64
<i>ATP2A2</i>	ATPase sarcoplasmic/endoplasmic reticulum Ca ²⁺ transporting 2	ER/mitophagy	65
<i>RETREG3</i>	Reticulophagy regulator family member 3	ER-phagy	66
<i>TEX264</i>	Testis expressed 264, ER-phagy receptor	ER-phagy	67
<i>UFL1</i>	UFM1 specific ligase 1	ER-phagy	23
<i>ATG9A</i>	Autophagy related 9A	Induction	34
<i>AUP1</i>	AUP1 lipid droplet regulating VLDL assembly factor	Induction	68
<i>CALR</i>	Calreticulin	Induction	69
<i>EIF4E</i>	Eukaryotic translation initiation factor 4E	Induction	70
<i>VMP1</i>	Vacuole membrane protein 1	Induction	71
<i>SPTLC1</i>	Serine palmitoyltransferase long chain base subunit 1	Induction/ER-phagy	72
<i>SPTLC2</i>	Serine palmitoyltransferase long chain base subunit 2	Induction/ER-phagy	72
<i>DDRGK1</i>	DDRGK domain containing 1	Lysosome	73
<i>LAMP2</i>	Lysosomal associated membrane protein 2	Lysosome	74
<i>PLAA</i>	Phospholipase A2 activating protein	Lysosome	75
<i>RIMOC1</i>	RAB7A interacting MON1-CCZ1 complex subunit 1	Lysosome fusion	76
<i>STX17</i>	Syntaxin 17	Lysosome fusion	77
<i>VAMP7</i>	Vesicle associated membrane protein 7	Lysosome fusion	78
<i>ATP5IF1</i>	ATP synthase inhibitory factor subunit 1	Mitophagy	79
<i>CERS1</i>	Ceramide synthase 1	Mitophagy	80
<i>FKBP8</i>	FKBP prolyl isomerase 8	Mitophagy	81
<i>FUNDC1</i>	FUN14 domain containing 1	Mitophagy	61
<i>PHB2</i>	Prohibitin 2	Mitophagy	82
<i>VCP</i>	Valosin containing protein	Mitophagy	83
<i>VDAC1</i>	Voltage dependent anion channel 1	Mitophagy	84
<i>HUWE1</i>	HECT, UBA and WWE domain containing E3 ubiquitin protein ligase 1	Mitophagy/mTOR	85
<i>GNAI3</i>	G protein subunit alpha i3	mTOR	86
<i>HK2</i>	Hexokinase 2	mTOR	87
<i>SCFD1</i>	Sec1 family domain containing 1	mTOR	88
<i>ATP6V0A1</i>	ATPase H ⁺ transporting V0 subunit a1	mTOR/Lysosome	89
<i>NPC1</i>	NPC intracellular cholesterol transporter 1	mTOR/Lysosome	90
<i>AMBRA1</i>	Autophagy and beclin 1 regulator 1	Regulation of autophagy	35
<i>BAG3</i>	BAG cochaperone 3	Regulation of autophagy	91
<i>CISD2</i>	CDGSH iron sulfur domain 2	Regulation of autophagy	92
<i>EIF4G1</i>	Eukaryotic translation initiation factor 4 gamma 1	Regulation of autophagy	93
<i>EMC6</i>	ER membrane protein complex subunit 6	Regulation of autophagy	94
<i>KEAP1</i>	Kelch like ECH associated protein 1	Regulation of autophagy	95
<i>MCL1</i>	MCL1 apoptosis regulator, BCL2 family member	Regulation of autophagy	96
<i>MTDH</i>	Metadherin	Regulation of autophagy	97
<i>S100A8</i>	S100 calcium binding protein A8	Regulation of autophagy	98
<i>TMEM39A</i>	Transmembrane protein 39A	Regulation of autophagy	99
<i>TMEM41B</i>	Transmembrane protein 41B	Regulation of autophagy	100
<i>TMEM59</i>	Transmembrane protein 59	Regulation of autophagy	101
<i>PIK3R2</i>	Phosphoinositide-3-kinase regulatory subunit 2	Upstream pathways	37
<i>PIK3R4</i>	Phosphoinositide-3-kinase regulatory subunit 4	Upstream pathways	37

Supplemental data

Supplemental Table S1. Upregulated genes identified by whole transcriptome sequencing of *Vlgr1*/del7TM retinae compared to WT retinae.

Supplemental Table S2. Downregulated genes identified by whole transcriptome sequencing of *Vlgr1*/del7TM retinae compared to WT retinae.